Upper Cenozoic chronostratigraphy of the southwestern Amazon Basin

Kenneth E. Campbell Jr.* Natural History Museum of Los Angeles County, 900 Exposition Boulevard, Los Angeles, California 90007, USA
Matt Heizler* New Mexico Bureau of Mines and Mineral Resources, 801 Leroy Place, Socorro, New Mexico 87801, USA
Carl D. Frailey Johnson County Community College, Overland Park, Kansas 66210, USA
Lidia Romero-Pittman Instituto Geológico, Minero y Metalúrgico (INGEMMET), San Borja, Apartado 889, Lima 41, Peru
Donald R. Prothero Department of Geology, Occidental College, Los Angeles, California 90041, USA

ABSTRACT

The lack of numerical age dates for upper Cenozoic strata of the Amazon Basin has prevented resolution of its geologic history and accurate dating of important paleofaunas. Here we present results of magnetostratigraphy and $^{40}Ar/^{39}Ar$ dating of two volcanic ash deposits from the Madre de Dios Formation of eastern Peru. The two ash ages, 9.01 ± 0.28 Ma and 3.12 ± 0.02 Ma, provide the first numerical age data necessary for accurate interpretation of late Tertiary sedimentation in Amazonia and establish approximate time constraints for the last major cycle of Cenozoic deposition within the southwestern Amazon Basin. The older ash age also provides a minimum age for numerous Amazonian paleofaunas, which allows a more definitive correlation of these paleofaunas with those in other regions of South America.

Keywords: Amazon Basin, argon-argon, chronostratigraphy, magnetostratigraphy, Miocene, Peru.

INTRODUCTION

The Cenozoic geologic history of the Amazon Basin remains controversial; interpretations of the origin, number, and ages of formations present are quite varied. Several regional, pre-Cenozoic subbasins and structural arches add to the overall stratigraphic complexity of the basin, and the complete lack of numerical age dates for any Cenozoic sedimentary deposit within the basin has delayed resolution of its geologic history. We present here results from two $^{40}Ar/^{39}Ar$ dates on volcanic ash deposits and magnetostratigraphy from eastern Peru that provide the first chronological anchors for interpreting the upper Tertiary Amazonian stratigraphy and late Tertiary paleofaunas of southwestern Amazonia. These results have broad application to understanding the geologic history of Amazonia if the Amazon Basin functioned as a single integrated sedimentary basin in the late Cenozoic, as has been proposed. In addition to facilitating the correlation of some Amazonian paleofaunas, the older ash age establishes the fact that at least one North American mammal was in South America more than 9 m.y. ago. This alters established interpretations regarding the timing of certain events associated with the Great American Faunal Interchange.

UPPER CENOZOIC STRATIGRAPHY OF AMAZONIA

The Amazon Basin is an elevated sedimentary basin in the process of being dissected by an entrenched river system. With possible limited exceptions (Neller et al., 1992; Dumont, 1993), all sediment carried into the basin is also carried out, although short-term residence as flood-plain deposits does occur (Mertes et al., 1996; Dunne et al., 1998). Some authors (Räsänen et al., 1987, 1990; Dumont, 1993) have suggested that regional subbasins were independently and differentially tectonically active in the late Cenozoic and as a consequence geologic formations cannot be correlated among these subbasins. These suggestions remain unsupported by direct geologic data, however, and we concur with the more traditional interpretation wherein two distinct Cenozoic stratigraphic intervals can be correlated throughout central and western Amazonia (Kummel, 1948; Schobbenhaus et al., 1984; Santos, 1974). The lower interval includes a Paleocene to upper Miocene sequence referred to as the Red Beds of the Contamana Group (Kummel, 1948) (Fig. 1). The formation at the top of this sequence in Peru is the upper Miocene Ipururo Formation (= Solimões Formation, in part, in Brazil [Schobbenhaus et al., 1984]). The Ucayali unconformity (Kummel, 1948) separates the older Tertiary deposits from the overlying sequence of younger deposits referred to in Peru as the Madre de Dios Formation (Oppenheim, 1946) (= Içá Formation in Brazil [Schobbenhaus et al., 1984]). The moderately to well consolidated, commonly faulted, and slightly dipping clay and mudstone horizons of the Ipururo Formation are readily distinguished from the unconsolidated, rarely faulted, horizontal sand, silt, and clay beds of the Madre de Dios Formation in central and southern Amazonian Peru.

The Ucayali unconformity is an excellent stratigraphic marker because it is very obvious and widespread. Three of us (Campbell, Frailey, and Romero-Pittman) have observed this unconformity from the foothills of the Peruvian Andes to the Brazilian Shield, throughout eastern Peru, northern Bolivia, and western Brazil. On the basis of descriptions by others, we conclude that it has been identified in well cores on both sides of the Amazon River (Maia et al., 1977) and in eastern Colombia (Hoorn et al., 1995). The ubiquity of this unconformity and the observed uniformity in the overlying stratigraphic sequence of the Madre de Dios Formation are taken as evidence documenting a common late Cenozoic geologic history throughout central and western Amazonia.

Although complex intraformational facies variations among the heterogeneous beds of unconsolidated clays, silts, and sands of the Madre de Dios Formation are common, our field data led us to divide the Madre de Dios Formation into three informal units (Fig. 1). A basal clay-pebble or clay-ball conglomerate locally rich in fossil vertebrates is typical of the oldest horizon of the formation, unit A. This facies was dated to the upper Miocene (Huayquerian South American Land Mammal Age [SALMA], or 9–6 Ma) on the basis of its contained fossil vertebrates (Frailey, 1986). Others, however, thought these fossils could be older (Chasicoan SALMA, or 12–9 Ma) (de Broin et al., 1993; Webb, 1995). The top of the upper horizon, unit C, forms the Amazon planalto (Sombroek, 1966), or highest terra firma, of lowland Amazonia. Recognizable throughout the basin, although extensively eroded locally, the planalto represents the upper limit of deposition within the basin. The middle horizon, unit B, is set off from the other two by distinctive changes in lithology that we interpret as unconformities.

MATERIALS AND METHODS

$^{40}Ar/^{39}Ar$ Dating

Two localized deposits of lithologically distinctive volcanic ash from within the Madre

*E-mail addresses: Campbell—kcampbel@nhm.org; Heizler—matt@nmt.edu.

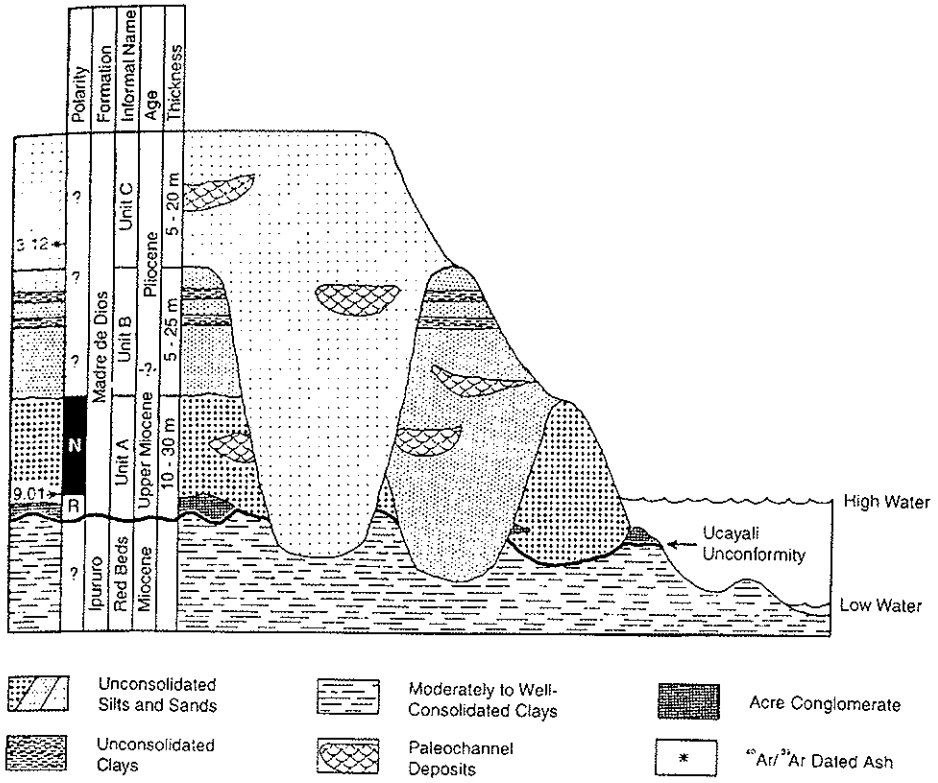

Figure 1. Generalized geologic section representing stratigraphic sequence commonly observed in riverine cutbanks in western and central Amazonia. Approximate, estimated stratigraphic positions of dated volcanic ashes and paleomagnetic samples shown are based on relative stratigraphic position in their respective outcrops. Although downcutting of younger horizons of Madre de Dios Formation through Ucayali unconformity as depicted here is theoretically possible, we have never observed downcutting on this scale in western Amazonia. The $^{40}Ar/^{39}Ar$ date on Cocama ash positions is within a zone of normal polarity, although it is within error of reversed chron C4Ar.1r.

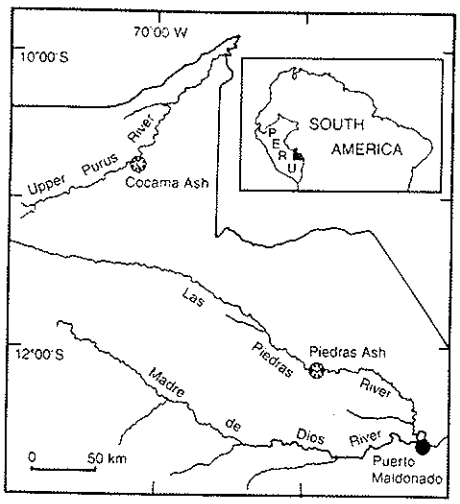

Figure 2. Map showing locations of Cocama and Piedras ash deposits.

de Dios Formation were dated by using $^{40}Ar/^{39}Ar$ techniques; the argon geochronology was conducted at the New Mexico Geochronology Research Laboratory. The Cocama ash, the older of the two, is a dense, fine-grained ash ~1.5 m thick that crops out over a distance of ~15 m just upstream from the mouth of the Cocama River, a small tributary of the Purus River (Fig. 2) (10°24′55″S, 71°10′22″W). The base of this ash is ~4 m above the Ucayali unconformity, which places it stratigraphically within the lower part of unit A of the Madre de Dios Formation.

The Piedras ash is a fine-grained ash deposit ~0.5 m thick that crops out over a lateral distance of ~35 m along the Las Piedras River (12°03′12″S, 69°54′06″W) in the same outcrop from which the magnetostratigraphic data were obtained (Fig. 2) (described subsequently). This locality is ~221 km south of the Cocama ash deposit. The ash came from low in unit C, the uppermost horizon of the Madre de Dios Formation. The ash samples were collected from large blocks at the base of the cliff, directly traceable to the source horizon above. The ash horizon is overlain by ~5 m of silts and clays that comprise the younger part of unit C. This outcrop is a cut into a minimally eroded part of the Amazon planalto; thus, the top of the section represents the highest level of Cenozoic deposition in this part of the basin. For the Piedras ash, both single- and bulk-grain laser-fusion analyses were conducted.

Minerals were removed from the ash samples by gentle crushing and dissolution of the matrix with 15% HF acid. K-feldspars ranging in diameter from 200 to 250 μm were obtained by heavy-liquid, magnetic, and hand-picking techniques. Samples were irradiated at the Texas A&M reactor for 7 h along with flux-monitor standard Fish Canyon Tuff sanidine (27.84 Ma). K-feldspar single and bulk grains were fused with the CO_2 laser, and the extracted gas was cleaned of reactive species for 2 min by using two SAES GP-50 getters (~400 and 20 °C), W filament (~2000 °C), and a cold trap (−140 °C). Extraction line blanks plus mass-spectrometer backgrounds were 120, 3, 0.5, 1.0, and 0.9 × 10^{-18} mol for masses 40, 39, 38, 37, and 36, respectively. Argon analyses were conducted with a MAP-215-50 mass spectrometer operated in static mode and an overall electron-multiplier sensitivity of 8 × 10^{-17} mol/pA. Automated gas handling, mass spectrometry, and age calculation were done by using software (Mass Spec v. 4.92) written by Al Denio, Berkeley Geochronology Center.

Magnetostratigraphy

For the purpose of determining magnetostratigraphy, the lower part of the Madre de Dios Formation was sampled at the locality on the Las Piedras River where the Piedras ash was collected. A series of 33 samples (11 sites, 3 samples per site) from ~2 m above the Ucayali unconformity and up through 19 m of section—i.e., all of unit A—was taken. The outcrop was a vertical cliff; the upper one-third was inaccessible, and thus sampling for magnetostratigraphy in units B and C was not possible. Unit thicknesses could not be measured directly, but at this outcrop, unit A is ~20 m, unit B is ~5 m, and unit C is ~6 m. The base of unit A was slightly underwater on this occasion.

The oriented samples were taken as blocks or, when the sediment was loose, in quartz glass jars sealed in the field. In the lab, the quartz glass jars were sealed with Zircar aluminum ceramic plugs. The samples were then analyzed following procedures outlined in Prothero and Britt (1998). Orthogonal demagnetization (Zijderveld) plots of representative samples showed very little response to AF demagnetization and considerable remanence above 600 °C. This result demonstrates that some high-coercivity, high-blocking-temperature mineral, such as hematite, is the primary carrier of the remanence in most samples. After AF demagnetization, most samples showed a clear stable remanence between 300 and 500 °C, which exhibited either normal or reversed polarity. This component was summarized by using the least-squares method of Kirschvink (1980) and averaged by using Fisher (1953) statistics.

Isothermal remanent magnetization (IRM) acquisition analysis showed that the samples were not saturated at 300 mT, but continued to acquire magnetization up to 1300 mT. Again, this result suggests that hematite is the primary carrier of the remanence. In representative lithologies, the ARM (anhysteretic remanent magnetization) was more resistant to AF demagnetization than the IRM, suggesting that the remanence is held in single-domain or pseudo–single-domain grains. Many samples had an obvious red stain, consistent with this interpretation.

RESULTS

$^{40}Ar/^{39}Ar$ Dating

Laser-fusion ages are arranged in increasing age order in Figure 3, and a running weighted mean and MSWD (mean squares of weighted deviates) are calculated (Table 1[1]). The youngest population (boxes in Table 1) that has an MSWD value within the 95% confidence window for $n - 1$ degrees of freedom is used as the best age of the sample.

To determine the age of the Cocama ash, 14 single crystals were analyzed; they yielded laser-fusion ages ranging from 6.0 ± 3.5 to 214.3 ± 1.0 Ma (Table 1; see footnote 1). The 10 youngest crystals are normally distributed and define a single population (MSWD = 1.0) with a calculated weighted mean age of 9.01 ± 0.28 Ma (Fig. 3A). The older crystals are thought to be xenocrysts. This date provides a minimum age for the beginning of deposition of the Madre de Dios Formation. A possible source for this ash is the very large Macusani volcanic field of the Peruvian Eastern Cordillera, ~460 km due south, older deposits of which have been dated at 9.4 ± 0.3 Ma (Noble et al., 1984).

The 26 single K-feldspar crystals from the Piedras ash that were analyzed yielded total fusion ages ranging from 2.7 to 7.2 Ma (Table 1); these have very high uncertainties because of the small argon signals associated with the small crystal size (~200 μm) and young age (Fig. 3B). The calculated radiogenic yields range from 72% to 172% and are positively correlated to the calculated apparent ages (Table 1; see footnote 1). The weighted mean age calculated from the 26 analyses is 3.92 ± 0.24 Ma, with an acceptable MSWD of 1.6 (Table 1). However, the large errors preclude identification of xenocrysts that might be slightly older than the true eruption age.

The large errors associated with the single-crystal analyses of the Piedras ash are directly tied to the inability to accurately measure ^{36}Ar in small crystals. ^{36}Ar is used to determine the atmospheric correction of the total measured ^{40}Ar. Pristine sanidine crystals that are relatively old (older than 1 Ma) are typically highly radiogenic. If a crystal is 100% radiogenic, the blank corrected $^{40}Ar/^{39}Ar$ measured ratio will yield the correct age of the sample.

The measured $^{40}Ar/^{39}Ar$ ratio is quite constant for the single crystals from the Piedras ash (Table 1; see footnote 1), which may indicate that the crystals are of equal age and have a constant radiogenic yield. Apparent ages for each single crystal were recalculated by assuming that they are 100% radiogenic; these are plotted in Figure 3C. The youngest 11 crystals yield a population that falls within the 95% confidence level for $n - 1$ degrees of freedom (Mahon, 1996) and gives a weighted mean age of 3.30 ± 0.03 Ma. This non–atmospheric-corrected date is interpreted to be a maximum age for the ash sample.

To overcome the low analytical precision associated with the small argon signals from the tiny single crystals of the Piedras ash, groups of ~30–50 grains were fused. The 14 bulk analyses range from ca. 3.1 to 4.4 Ma and are much more precise than the single-crystal ages (Fig. 3D, Table 1; see footnote 1). The six youngest age results from the bulk sample fusions are a normally distributed population (MSWD = 2.5) and yield a weighted mean of 3.12 ± 0.02 Ma (Table 1). This age is similar to the non–atmospheric-corrected age from the single crystals, and we conclude that it is the best estimate for the age of the ash sample. The scatter to older ages for some of the bulk analyses (Fig. 3D) is thought to be caused by xenocrystic contamination.

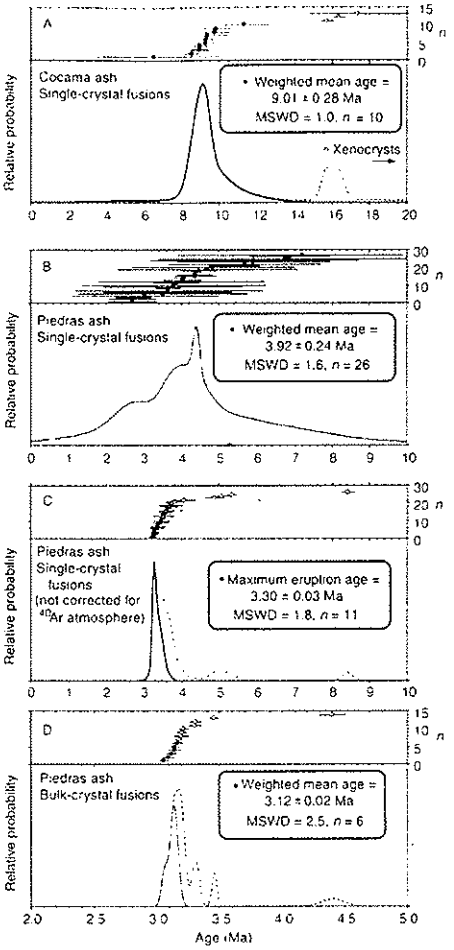

Figure 3. Probability distribution diagrams for $^{40}Ar/^{39}Ar$ age results. Individual age results are shown with 2 σ error bars. A: Cocama ash—the youngest 10 single crystals yield weighted mean age of 9.01 ± 0.28 Ma, which is interpreted to be eruption age. B: Piedras ash—single-crystal results yield calculated normal distribution. However, analytical error is too high to evaluate existence of xenocrystic contamination. C: Piedras ash—single-crystal ages calculated by assuming grains are 100% radiogenic. This calculation provides maximum age for ash of 3.30 ± 0.03 Ma; older apparent ages could be xenocrysts and/or lower radiogenic grains. D: Piedras ash—age distribution for bulk-grain analyses. Partly on the basis of single-crystal results that do not indicate extensive xenocrystic contamination, youngest population of bulk fusion ages (3.12 ± 0.02 Ma) is interpreted as eruption date of this ash.

Magnetostratigraphy

The mean for all normal sites was D = 355.3°, I = −18.3°, k = 16.0, α_{95} = 11.2; for reversed sites, D = 200.6°, I = 16.9°, k = 14.6, α_{95} = 24.8. These values are consistent with the present location of the sampling area. In addition, the normal and reversed directions are antipodal within error estimates. This positive reversal test shows that the directions are primary and that overprinting has been largely removed. The three resultant vectors for each site were averaged. All sites were considered significant (statistically distinguishable from random scatter at the 95% confidence interval). Results of the magnetic analyses are shown in Figure 1. We do not regard these results as the definitive magnetostratigraphy of unit A because they represent only one sampling traverse and the site spacing was coarse.

The lower two sample sites, positioned stratigraphically just below or overlapping the Cocama ash, have reversed magnetic polarity, whereas the remainder are normal. Reversed chron C4Ar.1r extends from 9.025 to 9.230 Ma (Berggren et al., 1995), which is within error of the 9.01 ± 0.28 Ma $^{40}Ar/^{39}Ar$ date for the Cocama ash. Thus, these results are consistent with that date.

DISCUSSION

It is not possible to document the geologic history of a region as vast as the Amazon Ba-

[1]GSA Data Repository item 2001065, Table 1, Isotopic results for laser-fusion analysis of both single- and multiple-crystal samples, is available on request from Documents Secretary, GSA, P.O. Box 9140, Boulder, CO 80301-9140, editing@geosociety.org, or at www.geosociety.org/pubs/ft2001.htm.

sin on the basis of $^{40}Ar/^{39}Ar$ results from only two geographically isolated ash deposits and one small series of magnetostratigraphic data. Nonetheless, these results do provide approximate time constraints for the last major cycle of Cenozoic deposition within the southwestern Amazon Basin. It should also be noted that our data from southwestern Amazonia correspond fairly closely to the age estimates for corresponding strata above the Ucayali unconformity given by Hoorn et al. (1995) for northwestern Amazonia. This correspondence supports the interpretation that the Amazon Basin was a single depositional basin in the late Cenozoic and that the capping strata within the basin are age equivalents.

The $^{40}Ar/^{39}Ar$ date on the Cocama ash corroborates the late Miocene age assignment for the paleofaunas from the basal conglomerates of the Madre de Dios Formation (Frailey, 1986; de Broin et al., 1993; Webb, 1995), which lie above the Ucayali unconformity but stratigraphically below the Cocama ash. These paleofaunas are commonly rich and highly diverse, including specimens of all vertebrate classes (Frailey, 1986; de Broin et al., 1993; Webb, 1995; Simpson and Paula Couto, 1981). Their minimum age established, these paleofaunas can now be correlated with those of other parts of South America with more precision.

The $^{40}Ar/^{39}Ar$ date on the Cocama ash also corroborates the preliminary late Miocene age assignment for *Amahuacatherium peruvium* (Romero-P., 1996), a tusked, brevirostrine gomphothere found in situ as a partial, articulated skeleton below the Ucayali unconformity in southeastern Peru (Frailey et al., 1997). From the fact that the Cocama ash lies ~4 m above the Ucayali unconformity, we estimate that this specimen of *Amahuacatherium peruvium* dates to at least 9.5 Ma, although it may be considerably older. This record is of some note because proboscideans were not previously thought to have arrived in South America from Central America until 2.0–1.9 Ma (Marshall, 1985).

Although the date of 3.12 ± 0.02 Ma (Table 1) from the Piedras ash marks a period near the end of the cycle of deposition that formed the Madre de Dios Formation, most of unit C was deposited after the ash horizon. Considering the amount and type of sediment accumulation after deposition of the Piedras ash, we estimate that deposition of the Madre de Dios Formation continued for some time, perhaps until the middle late Pliocene (ca. 2.5 Ma). It may be possible to corroborate this age estimate through the use of magnetostratigraphic data from the upper parts of the Madre de Dios Formation.

ACKNOWLEDGMENTS

We thank Michael Woodburne and Philip Gingerich for critical comments on an early draft of this manuscript and S. David Webb for his helpful comments on the final draft; J.L. Kirschvink for access to the Caltech paleomagnetics lab; and Hugo Rivera, Director Técnico, INGEMMET, for his enthusiastic collaboration and support. Field work was funded by the National Geographic Society and John G. Wigmore.

REFERENCES CITED

Berggren, W.A., Kent, D.V., Swisher, C.C., III, and Aubry, M.-P., 1995, A revised Cenozoic geochronology and chronostratigraphy: SEPM (Society for Sedimentary Geology) Special Publication 54, p. 129–212.

de Broin, F., Bocquentin, J., and Negri, F.R., 1993, Gigantic turtles (Pleurodira, Podocnemididae) from the late Miocene–early Pliocene of south western Amazon: Institut Français d'Études Andiennes, v. 22, p. 657–670.

Dumont, J.F., 1993, Lake patterns as related to neotectonics in subsiding basins: The example of the Ucamara Depression, Peru: Tectonophysics, v. 222, p. 69–78.

Dunne, T., Mertes, L.A.K., Meade, R.H., Richey, J.E., and Forsberg, B.R., 1998, Exchanges of sediment between the flood plain and channel of the Amazon River in Brazil: Geological Society of America Bulletin, v. 110, p. 450–467.

Fisher, R.A., 1953, Dispersion on a sphere: Royal Society of London Proceedings, v. A217, p. 295–305.

Frailey, C.D., 1986, Late Miocene and Holocene mammals, exclusive of the Notoungulata, of the Rio Acre region, western Amazonia: Natural History Museum of Los Angeles County Contributions in Science, no. 374, p. 1–46.

Frailey, C.D., Campbell, K.E., Jr., and Romero-P., L., 1997, A new proboscidean from Amazonian Peru, *in* Shoshani, J., and Tassy, P., eds., The Proboscidea: Evolution and palaeoecology of elephants and their relatives: Oxford, UK, Oxford University Press, Appendix 29.1, p. 295.

Hoorn, C., Guerrero, J., Sarmiento, G.A., and Lorente, M.A., 1995, Andean tectonics as a cause for changing drainage patterns in Miocene northern South America: Geology, v. 23, p. 237–240.

Kirschvink, J.L., 1980, The least-squares line and plane and the analysis of paleomagnetic data: Royal Astronomical Society Geophysical Journal, v. 62, p. 699–718.

Kummel, B., 1948, Geological reconnaissance of the Contamana region, Peru: Geological Society of America Bulletin, v. 69, p. 1217–1266.

Mahon, K.I., 1996, The new "York" regression: Application of an improved statistical method to geochemistry: International Geology Review, v. 38, p. 293–303.

Maia, R.G., Godoy, H.K., Yamaguti, H.S., de Moura, P.A., da Costa, F.S., de Holanda, M.A., and Costa, J., 1977, Projeto Carvão no Alto Solimões, Relatorio Final: Brasilia, Companhia de Pesquisa de Recursos Minerais-Departamento Nacional da Produção Mineral, 142 p.

Marshall, L.G., 1985, Geochronology and land-mammal biochronology of the transamerican faunal interchange, *in* Stehli, F.G., and Webb, S.D., eds., The great American biotic interchange: New York, Plenum Press, p. 49–85.

Mertes, L.A.K., Dunne, T., and Martinelli, L.A., 1996, Channel-floodplain geomorphology along the Solimões-Amazon River, Brazil: Geological Society of America Bulletin, v. 108, p. 1089–1107.

Neller, R.J., Kong, H., Salo, J.S., and Räsänen, M.E., 1992, On the formation of blocked valley lakes by channel avulsion in upper Amazon foreland basins: Zeitschrift für Geomorphologie N.F., v. 36, p. 401–411.

Noble, D.C., Vogel, T.A., Peterson, P.S., Landis, G.P., Grant, N.K., Jezek, P.A., and McKee, E.H., 1984, Rare-element-enriched, S-type ash-flow tuffs containing phenocrysts of muscovite, andalusite, and sillimanite, southeastern Peru: Geology, v. 12, p. 35–39.

Oppenheim, V., 1946, Geological reconnaissance in southeastern Peru: American Association of Petroleum Geologists Bulletin, v. 30, p. 254–264.

Prothero, D.R., and Britt, J.R., 1998, Magnetic stratigraphy and tectonic rotation of the middle Eocene Matilija Sandstone and Cozy Dell Shale, Ventura County, California: Implications for sequence stratigraphic correlations: Earth and Planetary Science Letters, v. 163, p. 261–273.

Räsänen, M.E., Salo, J.S., and Kalliola, R.J., 1987, Fluvial perturbance in the western Amazon Basin: Regulation by long-term sub-Andean tectonics: Science, v. 238, p. 1398–1401.

Räsänen, M.E., Salo, J.S., Jungnert, J., and Romero-Pittman, L., 1990, Evolution of the Western Amazon lowland relief: Impact of Andean foreland dynamics: Terra Nova, v. 2, p. 320–332.

Romero-P., L., 1996, Paleontología de Vertebrados, *in* Palacios-M., O., et al., eds., Geología de los cuadrangulos de Puerto Luz, Colorado, Laberinto, Puerto Maldonado, Quincemil, Masuco, Astillero y Tambopata: Instituto Geológico Minero y Metalúrgico, Carta Geológica Nacional, Boletín, ser. A, no. 81, p. 171–178.

Santos, J.O.S., 1974, Considerações sobre a bacia cenozõica Solimões: Sociedade Brasileira de Geologia, Anais do XXVIII Congresso, v. 3, p. 3–11.

Schobbenhaus, C., de Almeida Campos, D., Derze, G.R., and Asmus, H.E., editors, 1984, Geologia do Brasil: Brasilia, Departamento Nacional da Produção Mineral, 501 p.

Simpson, G.G., and Paula Couto, C., 1981, Fossil mammals from the Cenozoic of Acre, Brazil, III—Pleistocene Edentata Pilosa, Proboscidea, Sirenia, Perissodactyla and Artiodactyla: Iheringia, sér. Geologia, v. 6, p. 11–73.

Sombroek, W.G., 1966, Amazon soils: Wageningen, Holland, Centre for Agricultural Publications and Documentation, 292 p.

Webb, S.D., 1995, Biological implications of the middle Miocene Amazon seaway: Science, v. 269, p. 361–362.

Manuscript received November 3, 2000
Revised manuscript received March 1, 2001
Manuscript accepted March 9, 2001

Printed in USA